Electronic Supplementary Information (ESI)

High-performance ternary organic solar cells with thick active layer exceeding 11% efficiency

Nicola Gasparini[1], Luca Lucera[2], Michael Salvador[13], Mario Prosa[4], George D. Spyropoulos[4], Peter Kubis[2], Hans-Joachim Egelhaaf[2], Christoph J. Brabec[1,5] and Tayebeh Ameri[1]

[1]Institute of Materials for Electronics and Energy Technology (I-MEET), Friedrich-Alexander-University Erlangen-Nuremberg, Martensstraße 7, 91058 Erlangen, Germany

[2]ZAE Bayern – Solar Factory of the Future, Energy Campus Nurnberg, Furtherstrasse 250, 90429 Nurnberg, Germany.

[3]Instituto de Telecomunicações, Instituto Superior Técnico, Av. Rovisco Pais, P-1049-001 Lisboa, Portugal

[4]Consiglio Nazionale delle Ricerche (CNR) - Istituto per lo Studio dei Materiali Nanostrutturati (ISMN), Via P. Gobetti, 101, 40129 Bologna, Italy

[5]Bavarian Center for Applied Energy Research (ZAE Bayern), Haberstrasse 2a, 91058 Erlangen, Germany

Email: nicola.gasparini@fau.de; tayebeh.ameri@fau.de

Table S1.Photovoltaic device parameters of PBTZT-STAT-BDTT-8:PTB7-th:$PC_{70}BM$ inverted solar cells under 1 sun illumination (100 mW cm^{-2}). The statistics is based on 18 solar cells.

PBTZT-STAT-BDTT-8:PTB7-th:$PC_{70}BM$	***Area*** **[mm^2]**	***V_{oc}*** **[V]**	***J_{sc}*** **[mA cm^{-2}]**	***FF*** **[%]**	***PCE*** **[%]**
1:0:1.5	10.4	0.78 (0.78±0.01)	16.68 (16.39±0.19)	67.08 (66.70±0.28)	8.64 (8.16±0.44)
0.75:0.25:1.5	10.4	0.77 (0.77±0.01)	17.61 (16.25±1.09)	71.13 (70.33±0.73)	9.64 (9.05±0.61)
0.5:0.5:1.5	10.4	0.77 (0.77±0.01)	18.67 (18.53±0.08)	71.07 (70.58±0.76)	10.21 (10.06±0.14)
0.25:0.75:1.5	10.4	0.77 (0.77±0.01)	18.16 (17.37±0.84)	67.72 (66.94±0.55)	9.46 (8.99±0.57)
0:1:1.5	10.4	0.77 (0.77±0.01)	15.92 (15.57±0.28)	69.13 (68.47±0.47)	8.66 (8.33±0.20)

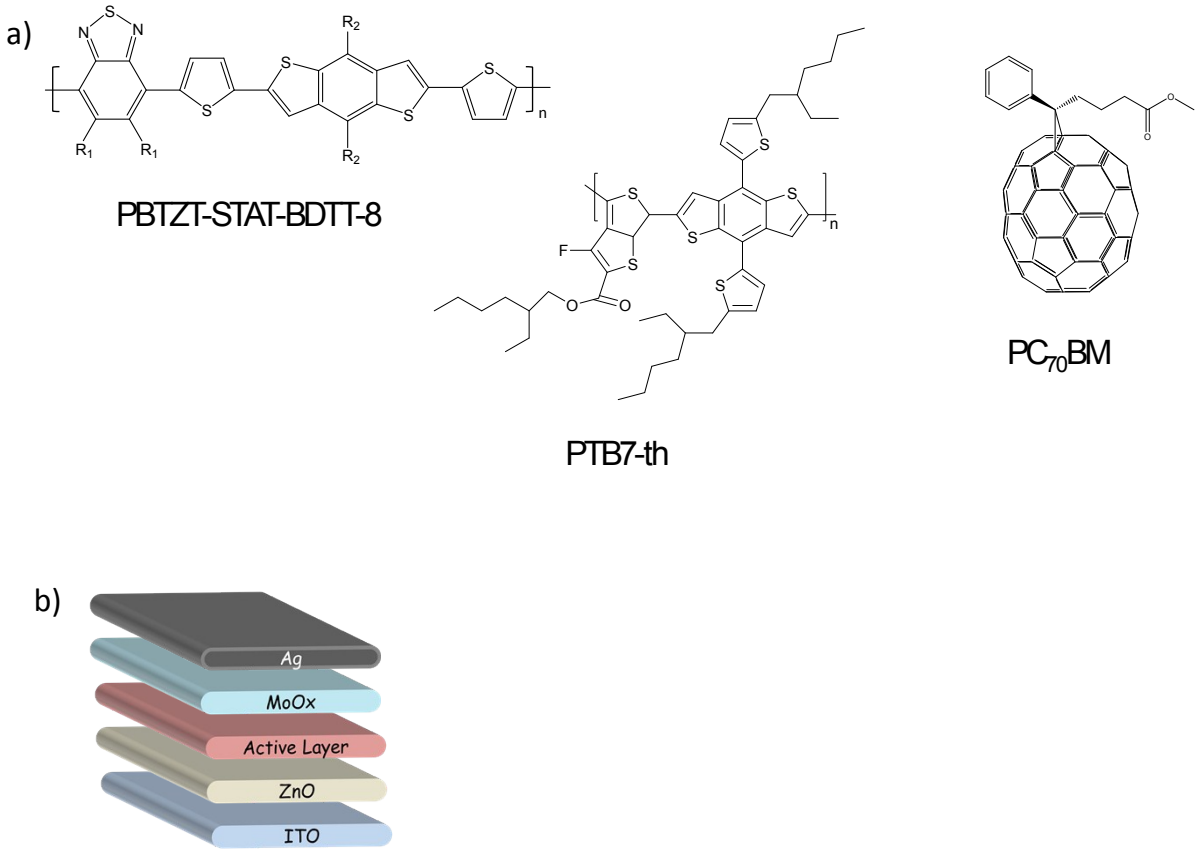

Figure S1 Molecular structures of the polymers and the fullerene derivative used in this work (a) and solar cells layout (b).

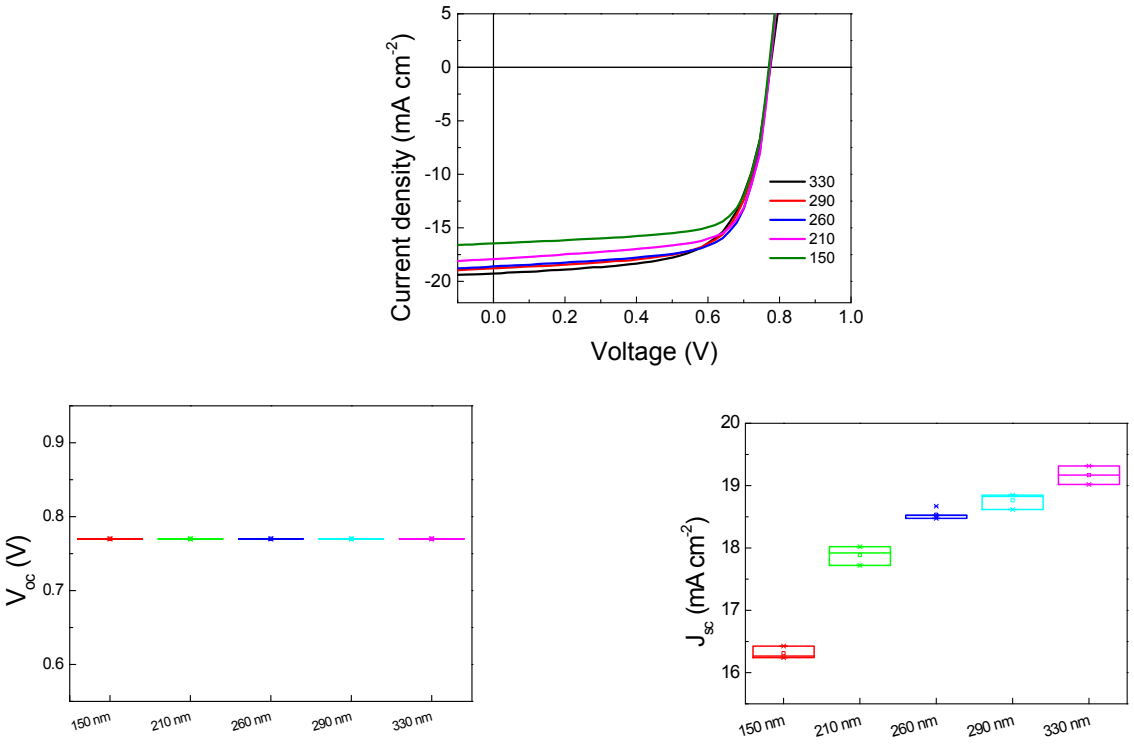

Figure S2 a) Current-voltage characteristics of PBTZT-STAT-BDTT-8:PTB7-th:$PC_{70}BM$ devices with different blend thicknesses. b) and c) V_{oc} and J_{sc} box plots for ternary devices, respectively.

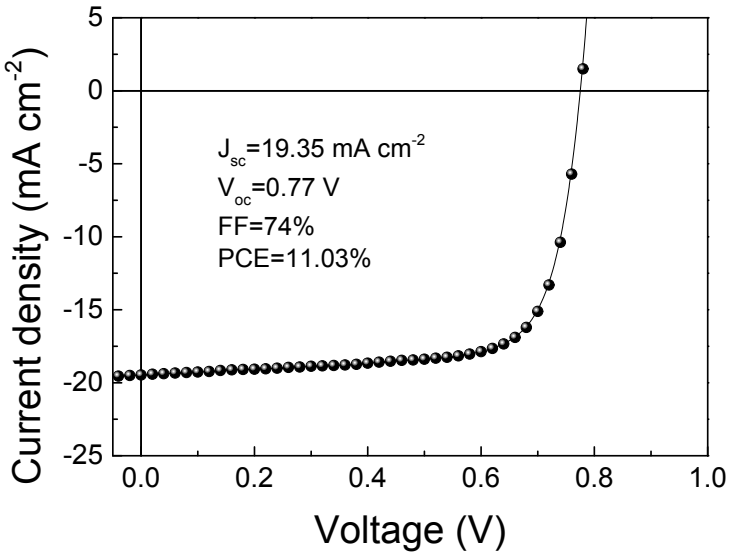

Figure S3 Current-voltage characteristics of PBTZT-STAT-BDTT-8:PTB7-th:$PC_{70}BM$ (0.5:0.5:1.5) champion device with an active area of 2 mm^2.

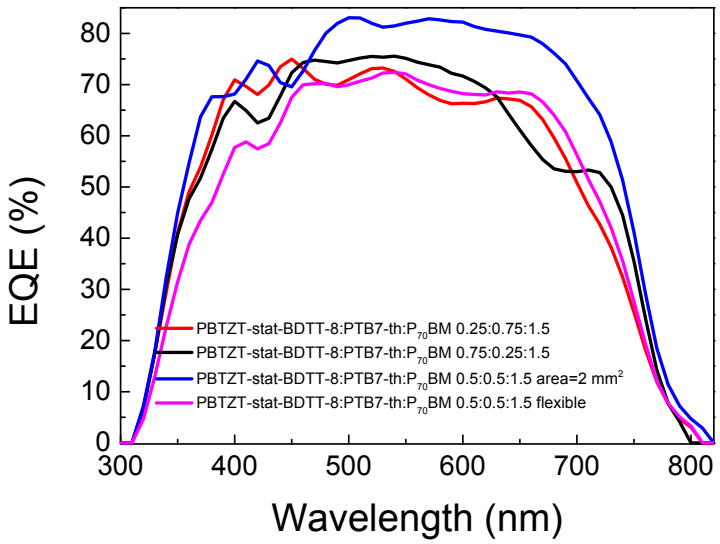

Figure S4 External quantum efficiency measurements of ternary blends.

Table S2 Comparison of short circuit current values extracted from current-voltage characteristics and EQE measurements.

PBTZT-STAT-BDTT-8:PTB7-th:$PC_{70}BM$	J_{sc} **[mA cm^{-2}]**	J_{sc} **(EQE) [mA cm^{-2}]**
1:0:1.5	16.68 (16.39±0.19)	15.85
0.75:0.25:1.5	17.61 (16.25±1.09)	16.38
0.5:0.5:1.5	18.67 (18.53±0.08)	18.12
0.5:0.5:1.5 2 mm^2	19.35 (19.17±0.15)	18.61
0.25:0.75:1.5	18.16 (17.37±0.84)	16.98
0:1:1.5	15.92 (15.57±0.28)	15.52
0.5:0.5:1.5 on IMI	15.2 (14.93±0.24)	14.49

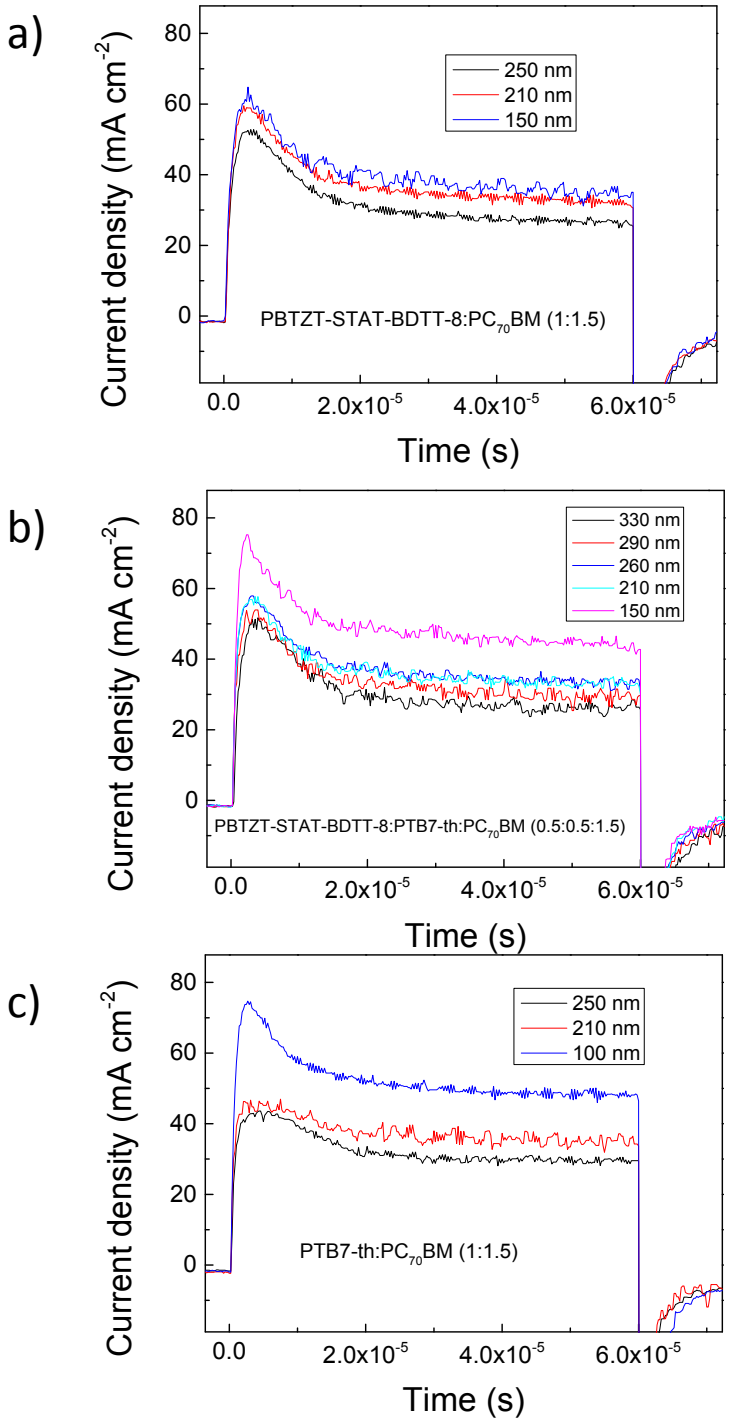

Figure S5 Photo-CELIV traces for binary and ternary devices with different active layer thicknesses.

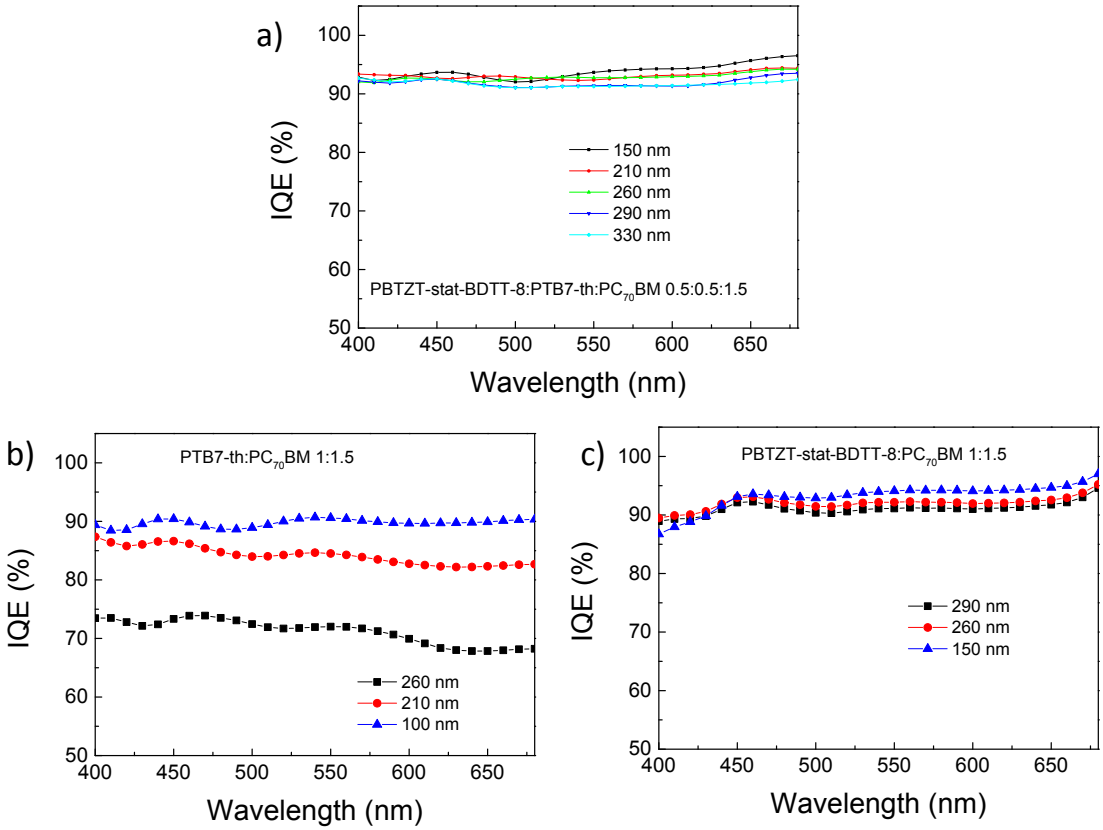

Figure S6 IQE spectra of PBTZT-STAT-BDTT-8:PTB7-th:$PC_{70}BM$, of PBTZT-STAT-BDTT-8: $PC_{70}BM$ and of PTB7-th:$PC_{70}BM$ as a function of the blend thickness.

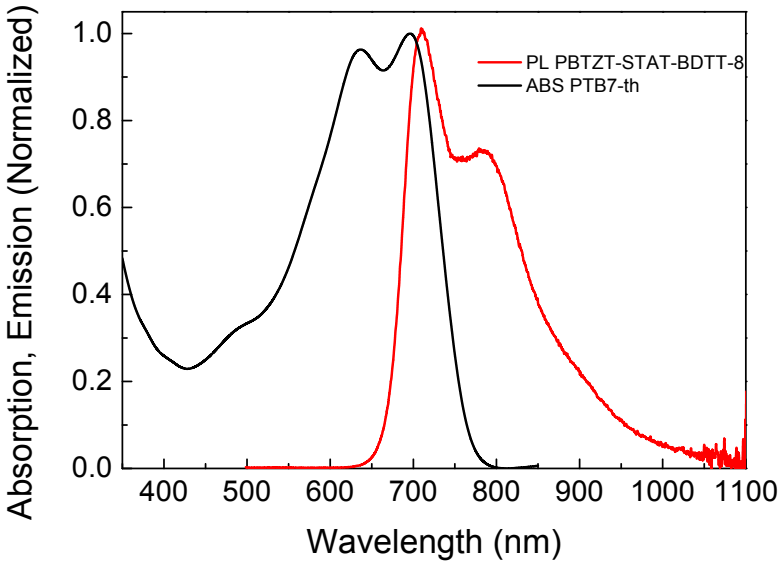

Figure S7 Absorption spectrum of a PTB7-th film and emission profile of a PBTZT-STAT-BDTT-8 film on glass.

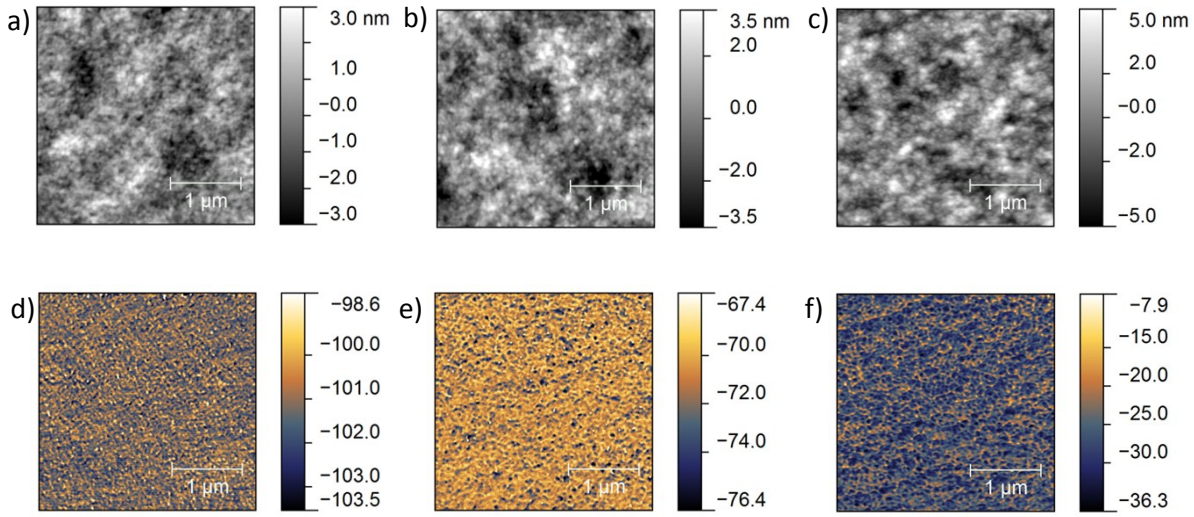

Figure S8 Topography and phase images of PBTZT-STAT-BDTT-8:$PC_{70}BM$ (a and d), PBTZT-STAT-BDTT-8:PTB7-th:$PC_{70}BM$ (b and e) and PTB7-th:$PC_{70}BM$ (c and f), respectively.

Table S3 Laser parameters used for P1, P2 and P3 lines.

Layer	Laser Fluence [J/cm2]	Overlap [%]	Repetitions over same line
ITO	0,35	97,45	3x
IMI	0,42	57,45	1x
Absorber	0,08	93,62	3x
Ag 150 nm	0,58	81,70	1x
Ag 100 nm	0,43	74,47	1x